AIAA 81-1553R

An Improved Model for the Combustion of AP Composite Propellants

Norman S. Cohen* and Leon D. Strand†
Jet Propulsion Laboratory, California Institute of Technology, Pasadena, California

This paper presents several improvements in the Beckstead-Derr-Price model of steady-state burning of AP composite solid propellants. The Price-Boggs-Derr model of AP monopropellant burning is incorporated to represent the AP. A separate energy equation is written for the binder to permit a different surface temperature from the AP. The discussion includes an analysis of the sharing of primary diffusion flame energy and a correction in treating the binder regression rate. A method for assembling component contributions to calculate the burning rates of multimodal propellants is also presented. Results are shown in the form of representative burning rate curves, comparisons with data, and calculated internal details of interest. Ideas for future work are discussed in an Appendix.

Nomenclature

a = kinetics constant for the oxidizer monopropellant flame
A_{AP} = kinetics prefactor for the oxidizer monopropellant flame reaction
A_{fh} = average flame height factor with respect to the oxidizer
A_{ox} = kinetics prefactor for oxidizer surface decomposition
A_s = kinetics prefactor for subsurface condensed-phase reactions
b = surface characteristic dimension, Eq. (19)
B_{fh} = average flame height factor with respect to the binder
c_g = specific heat of oxidizer combustion product gases
c_s = specific heat of the solid
D = oxidizer particle size
E_{AP} = activation energy for the oxidizer monopropellant flame reaction
E_{ox} = activation energy for oxidizer surface decomposition
E_s = activation energy for subsurface condensed-phase reactions
$(h/D)_{P,N}$ = height of particle protrusion or depression relative to the positive or negative intersecting binder surface plane
ΔH_{ev} = oxidizer heat of vaporization at 298 K
ΔH_g = latent heat of oxidizer decomposition products
ΔH_s = latent heat of the solid oxidizer
m_f = mass flux of binder
m_{ox} = mass flux of oxidizer
m_T = summation of mass flux defined by Eq. (14)
O/F = oxidizer/binder ratio
$(O/F)^*$ = oxidizer/binder ratio of a pseudopropellant
P = pressure
Q_f = heat of binder decomposition
Q_F = heat content of adiabatic oxidizer monopropellant flame
Q_L = net heat release at the oxidizer surface
Q_{ox} = heat release in the oxidizer monopropellant flame
Q_{PF} = heat release in the primary diffusion flame
R = universal gas constant
r = burning rate
r_f = binder regression rate
r_{ox} = oxidizer regression rate
S_f = binder surface area
S_0 = total surface area
S_{ox} = oxidizer surface area
T_0 = propellant conditioning temperature
T_{ox} = oxidizer monopropellant flame temperature, function of P and T_0
T_s = oxidizer surface temperature
T_{sf} = binder surface temperature
V_j = pseudopropellant volume per unit propellent volume
X_D^* = mixing length for diffusion flame
X_{ox}^* = flame standoff distance at which Q_{ox} is released
X_{PDF}^* = flame standoff distance at which Q_{PF} is released over the oxidizer
X_{PDFf}^* = flame standoff distance at which Q_{PF} is released over the binder
X_{PF}^* = reaction length for diffusion flame
α_f = binder weight fraction in the propellant
α_f^* = binder (fuel) weight fraction in the pseudopropellant, as apportioned
α_{fe} = weight fraction of binder (fuel) not reacted and available as excess for the next pseudopropellant
α_{fr} = weight fraction of binder that is reacted
α_{ox} = weight fraction of oxidizer of a particular size in the propellant
β_F = fraction of oxidizer that enters into the diffusion flame reaction to heat the oxidizer
β_{ox} = fraction of oxidizer that is used to heat the oxidizer
β_p = fraction of oxidizer not involved in condensed phase reactions
δ_{AP} = reaction order, oxidizer monopropellant flame reaction
ϕ = stoichiometric oxidizer/fuel ratio
λ_g = gas thermal conductivity
ρ_f = binder density
ρ_{ox} = oxidizer density
ρ_p = propellant density
ξ_{ox} = dimensionless flame height, oxidizer flame
ξ_{PF} = dimensionless flame height, primary flame situated over the oxidizer

Presented as Paper 81-1553 at the AIAA/SAE/ASME 17th Joint Propulsion Conference, Colorado Springs, Colo., July 27-29, 1981; submitted Aug. 31, 1981; revision received March 22, 1982.

*Contractor, Cohen Professional Services, Inc., Redlands, Calif. Member AIAA.
†Member of the Technical Staff. Associate Fellow AIAA.

ξ_{PFf} = dimensionless flame height, primary flame situated over the binder
ζ_f = volume fraction of binder
ζ_{ox} = volume fraction of oxidizer

Introduction

THE Beckstead-Derr-Price (BDP) model[1] of the steady-state burning of ammonium perchlorate (AP) composite propellants has provided a framework for various modeling efforts since its publication. These efforts have been reviewed for Cohen,[2] who pointed out a number of areas of needed improvement. The more important of these are discussed in this paper.

A latent deficiency in the BDP model is its inability to predict the shape of the burn rate curve of AP propellants at high pressure. By high pressure, in terms of the model, is meant the regime in which heat feedback from the AP flame is dominant. This regime moves to lower pressure with increasing particle size and decreasing solids loading. Most calculations have been within the regime of diffusion flame control, so the problem has not been of concern until recently. The problem arises because the simple BDP model for the AP monopropellant contains no pressure-dependent heat release, and the AP flame assumes the full burden of heating the propellant at high pressure. The result is the prediction of an asymptotic high-pressure burn rate with the pressure exponent approaching zero, rather than the observed inflection to a high exponent.

The Price-Boggs-Derr (PBD) model[3] of AP monopropellant combustion is a more comprehensive treatement than that used by BDP.[4] It contains pressure-dependent heat release, which is deemed helpful to the high-pressure problem. One task of this work was to incorporate that model to represent the AP.

An inconsistency in the BDP model is the use of two binder regression rates: one determined by an Arrhenius equation at the surface temperature of the AP and used to calculate the propellant surface structure and one determined by continuity to calculate the propellant burning rate. The inconsistency follows from the assumption of a uniform surface temperature. This assumption is now generally discredited. The assumption fostered the additional problem of computing unrealistic surface structures because the binder regression rates for the surface structure analysis were much too low. A second task was to correct this inconsistency.

The need for a separate surface temperature implies the need for a separate energy balance for the binder. A criticism of the BDP model has been that the binder was given too subordinate a role because it was made to simply follow along with the AP. A related problem is the fact that the heating of the binder is implied rather than expressed—there is no direct mechanism for heating the binder because the flames are viewed as being situated over the AP. Beckstead[5,6] has written a separate energy balance for the binder, but his method of apportioning heat feedback from the flame between the AP and binder is too simplified. A third objective of this work was to construct a separate energy balance for the binder, which included a model for direct heating. It turns out that this improved treatment is also helpful to the high-pressure problem.

A number of methods for treating and assembling component contributions to calculate the burning rates of multimodal propellants have been proposed.[2] All are based on some sort of averaging method. All are reported to successfully predict the size distribution effects on the burning rate, with the exception of propellants containing both very fine and very coarse AP ("wide-distribution propellants"). A fourth task was to explore new combination methods. The ability to predict the behavior of wide-distribution propellants as well as more conventional propellants was established as a goal that would verify the generality of the approach.

The purpose of this paper is to present the work which has been accomplished in these areas.

Monomodal Propellant Model

AP Monopropellant Model

The Price-Boggs-Derr model, as published, was not in a form suitable for convenient incorporation into the composite propellant model. To facilitate such incorporation, Price and Boggs distributed a memorandum[7] which presented their model in a compatible form. The following is a presentation of the revised model which was incorporated here.

Mass flux is given by

$$m_{ox} = \rho_{ox} r_{ox} = A_{ox} \exp(-E_{ox}/RT_s) \tag{1}$$

Given a trial T_s, the fraction of AP reacted in the gas phase is known from

$$\beta_p = 1 - \frac{A_s \exp(-E_s/RT_s)}{m_{ox}} \tag{2}$$

The remainder of the AP reacts in the condensed phase. Equation (2) assumes that the condensed-phase reactions may be lumped into an infinitesimally thin surface layer. The heat content of the adiabatic AP flame is

$$Q_F = c_g(T_{ox} - 298) - c_s(T_0 - 298) + \Delta H_g \tag{3}$$

The net surface heat term is

$$Q_L = \beta_p(\Delta H_{ev} - \Delta H_g) - (1 - \beta_p) Q_F \tag{4}$$

Thus the net heat release in the AP flame is given by

$$Q_{ox} = Q_F + Q_L = \beta_p [c_g(T_{ox} - 298) - c_s(T_0 - 298) + \Delta H_{ev}] \tag{5}$$

The flame standoff distance is expressed in the following parametric form, which is numerically equivalent to an effective result for heat feedback derived from the formal distributed reaction model,[3]

$$X^*_{ox} = \frac{m_{ox}}{a + A_{AP} \exp(-E_{AP}/RT_{ox}) P^{\delta_{AP}}} \tag{6}$$

The dimensionless standoff is

$$\xi_{ox} = (c_g/\lambda_g) m_{ox} X^*_{ox} \tag{7}$$

Finally, the heat balance at the surface is written for T_s as

$$T_s = T_0 - (Q_L + \Delta H_s)/c_s + (Q_{ox}/c_s) \exp(-\xi_{ox}) \tag{8}$$

This T_s is compared to the trial T_s and iterated to convergence.

Functional forms and values for the various input parameters may be obtained from the authors. Calculated results are shown in Table 1. The calculated burn rates are in agreement with data, and the calculated results were verified to be in agreement with those provided in the referenced memorandum.

Separate Energy Balance

The energy balance for the binder is

$$m_f S_f [c_s(T_{sf} - T_0) + Q_f] = (1 - \beta_{ox})(m_{ox} S_{ox} + m_f S_f) Q_{PF} \exp(-\xi_{PFf}) \tag{9}$$

Table 1 Calculated results for AP monopropellant combustion

Pressure, MPa	Burning rate, cm/s	Surface temperature, K	β_p	Flame height, μm	Q_L,[a] cal/g	Q_{ox}, cal/g
2.15	0.287	865.6	0.761	8.72	185.8	637.9
3.83	0.471	869.9	0.783	5.24	203.1	658.2
6.80	0.811	874.8	0.806	2.93	221.0	679.1
12.11	1.451	880.1	0.828	1.59	237.7	699.0
21.50	2.605	885.5	0.848	0.86	252.7	717.1

[a] Values of Q_L are endothermic.

The left side of the equation consists of energy required to heat the binder to its surface temperature, including the heat of decomposition. The right side consists of the fraction of primary diffusion flame energy that is utilized to heat the binder. The source of this energy is at an effective flame height that is different from that over the AP.

The energy balance for the AP is

$$m_{ox}S_{ox}[c_s(T_s-T_0)+\Delta H_s+Q_L] = \beta_{ox}\beta_F(m_{ox}S_{ox}+m_fS_f)Q_{PF}\exp(-\xi_{PF}) + \beta_{ox}(1-\beta_F)m_{ox}S_{ox}Q_{ox}\exp(-\xi_{ox}) \quad (10)$$

Equation (10) is Eq. (8) modified by the presence of the diffusion flame. It is used to calculate T_s and is the final step in the iteration as in the BDP model. Equations (9) and (10) contain an important assumption, namely that the portion of the diffusion flame that extends over the binder is not a part of the BDP competing flame process. Only the part that is over the AP is involved in this process. The assumption is on a sound geometric basis and is required in order to maintain the heating of the binder when the AP flame becomes controlling over the AP particle. Thus, β_F is not involved in Eq. (9). It should be noted that the final flame of the BDP model has been omitted. There have been conceptual problems associated with it and, as used, it has not contributed significantly to the energy balance.

Binder Regression Rate

The binder regression rate is specified by continuity of the formulation

$$m_fS_f = m_{ox}S_{ox}\alpha_f/\alpha_{ox} \quad (11)$$

$$r_f = m_f/\rho_f \quad (12)$$

This regression rate is used in the surface area calculations to determine S_{ox}. Unlike the BDP model, it must now be done in an iteration because r_f is a function of S_{ox} in this calculation. The regression rate is then used to determine T_{sf} from an Arrhenius decomposition law. T_{sf} then feeds into Eq. (9) to determine β_{ox}. Thus, r_f is used consistently in the model and $T_{sf} \neq T_s$.

Flame Heights

The BDP model has used an approximation of the Williams/Burke-Schumann diffusion flame analysis to determine an effective diffusion flame height over the AP. This approximation has been referred to as the "short flame assumption." The associated flame shape is an inverted parabola, closing over the AP without any projection over the binder. This shape corresponds to the "underventilated flame" solution,[8] applicable to fuel-rich mixtures typical of composite propellants. There are other flame shapes which result from the general solution. The original paper[8] gives examples of a billowed flame, where the flame initially projects over the fuel near the base of the flame before turning back to close over the oxidizer. For oxidizer-rich systems, the "overventilated flame" solution provides a shape that extends only over the fuel. The oxidizer-rich flame is of dubious relevance to composite propellants, but Beckstead[6] and others[2] have developed an argument for its possible existence in multimodal propellants. Multiple flame locations have also been extracted from the general model[9] and a phalanx flame shape (extending over both fuel and oxidizer) has been proposed from time to time.[10,11] Thus, there are bases for assuming that at least a portion of the diffusion flame extends over the binder. It is agreed that there is more to be learned about diffusion flame structure in composite propellants.[9]

Flame shape calculations were not performed in the course of this work. What has been done is to assume the applicability of the BDP model as far as the AP is concerned, and then to apply a different average flame height factor to represent the diffusion length with respect to the binder. The diffusion flame height over the binder is then expressed in the same form as that over the AP,

$$X^*_{PDFf} = X^*_{PF} + B_{fh}X^*_D \quad (13)$$

It turns out that the factor B_{fh} is much smaller than A_{fh}, the average flame height factor with respect to the AP. Thus the binder is heated by a relatively close-in flame, which is consistent with Burke-Schumann model solutions for flames which extend over the fuel.

In calculating X^*_D, the BDP expression of the characteristic surface dimension b has been replaced by one derived by Glick and Condon [see discussion in the review paper[2] and Eq. (19) later in this paper]. It is of more general validity, in particular for modeling multimodal propellants. Following the short-flame assumption, the diffusion length is proportional to this dimension. This work has retained the BDP approximation for the proportionality. It is a good approximation as long as one does not encounter large variations in O/F ratio or cross over to the oxidizer-rich side of stoichiometry. Beckstead[6] has recently provided simple parametric expressions for the proportionality that are more general and can be used in future work.

In calculating X^*_{PF}, the kinetics rate constant is written in an Arrhenius form to account for the temperature dependence. There are versions of the model that use a constant value for the rate constant. It is found that it is important to account for the temperature dependence.

Results of Burning Rate Calculations

The propellant formulations of King[12,13] were utilized to evaluate the model as applied to monomodal AP propellants (nonaluminized, HTPB binder). These propellants are good choices because they encompass a range of particle sizes and two AP concentrations at one size, which test different aspects of the model. Calculated burning rate curves are shown together with corresponding experimental data in Fig. 1. Agreement with data is very good in all cases.

The 5 μm AP propellant is calculated to be in the regime of primary diffusion flame control over most of the pressure range shown.‡ The slightly downward inflection in the curve is a characteristic of that regime. The transition to AP flame control is picked up by the transition to an upward inflection in the curve at about 10 MPa. The 20 μm AP propellants transition to AP flame control at about 3.5 MPa. Thus the pressure range shown is more equally distributed between diffusion flame control and AP flame control for those cases. The higher burning rate and greater curvature for the 77% AP propellant are due to the higher flame temperature and shorter reaction distance (X^*_{PF}). The importance of X^*_{PF} also appears in the higher exponent of the 5 μm propellant and in the merger of the low-pressure burn rates of the 5 and 20 μm

‡In terms of the current model, "diffusion flame control" or "AP flame control" now refers to the heat feedback to the AP rather than the propellant as a whole.

(73% AP) propellants. The 200 μm AP propellant is completely in the regime of AP flame control over this pressure range. This prediction is particularly satisfying because the prediction with the BDP model bore no similarity to the data.[2] The upward inflection that is characteristic of AP flame control is seen to be followed by a downward inflection at the high-pressure end. This downward inflection is due to increasing binder heating requirements through the β_{ox} parameter. Based on these results, it appears that the objective of improving the model capabilities at high pressure has been met.

Some of the calculated internal details of interest are shown in Table 2. The calculated surface temperatures of the AP are consistent with those in Table 1. Adding a binder to the system and a primary diffusion flame to the AP energy balance did not produce radical excursions in the surface temperature. Thus the model is well behaved. The binder surface temperatures are higher, as expected, but are beginning to exceed the regime of the experiments[14] performed to determine the binder kinetics and energetics. The mechanism and kinetics of binder decomposition may change at surface temperatures above about 1300 K. Table 2 includes the $(h/D)_N$ and β_{ox} parameters for the three particle sizes. All values of $(h/D)_P$ are pegged at the -0.212 limiting value. A problem with the BDP model is that all $(h/D)_N$ would also be pegged at its -0.788 limiting value. This is now corrected because the proper regression rate of the binder is utilized. The values of $(h/D)_N$ tend to become more positive with increasing particle size and decreasing pressure, which is the expected trend. The pressure effect is small for the finer particles. The value of β_{ox} is observed to increase with particle size and pressure, except that it starts to decrease at high pressure with the coarse AP. Competing factors determining β_{ox} are the binder surface temperature and the diffusion flame height over the binder. The trend has a significant effect upon the shape of the burning rate curve at high pressure; the regime of AP flame control should therefore be subdivided into a regime of increasing β_{ox} and one of decreasing β_{ox}. On the average, roughly 30% of the energy is being used to heat the binder; variations depart somewhat from the binder weight fraction. Based on these results, it appears that improved values for the surface parameters have been achieved and that the binder has a more significant role than in previous models.

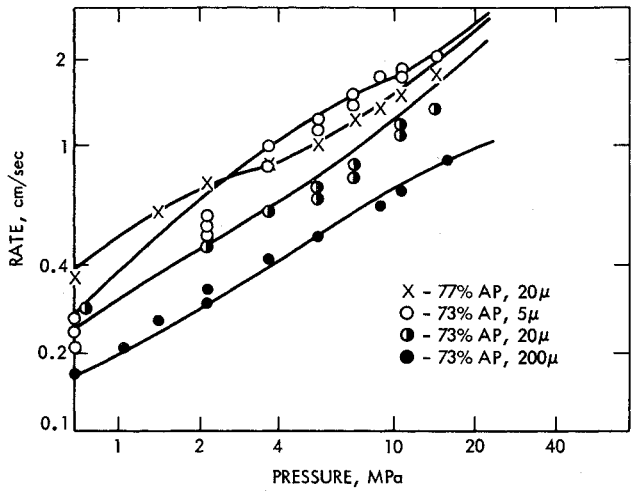

Fig. 1 Comparisons of model and data for King's monomodal propellants.

Calculated flame height components are shown in Table 3. The diffusion height is independent of pressure or burn rate. This remains true in Beckstead's recent expressions.[6] The relative importance of the reaction length (X^*_{PF}) in finer particle size propellants and at lower pressures is noteworthy. The flame standoff distances for the AP flame are comparable to Table 1 values at comparable pressures; they are a bit larger here because of the higher values for m_{ox}.

Multimodal Propellant Model

Several approaches were explored for building up the component modal contributions to express the aggregate propellant burning rate. The approach that was most successful is presented here. It did not, however, successfully predict effects observed in wide-distribution propellants. Attempts to address wide-distribution propellants are presented in the Appendix in order to provide ideas and commentary that might be useful for future work.

Propellant Buildup Relations

The approach adopted is a variation of the Glick and Condon "petit ensemble model." In that model (see the review paper[2]), each modal component is viewed as a separate and independent "pseudopropellant." Each pseudopropellant includes an assigned portion of binder. The burning

Table 2 Calculated internal quantities for King's 73% AP-HTPB propellants

Pressure, MPa	Surface temperature, K AP 20μmAP	Surface temperature, K HTPB 20μmAP	Surface structure, $(h/D)_N$ 5μm	Surface structure, $(h/D)_N$ 20μm	Surface structure, $(h/D)_N$ 200μm	Diffusion flame energy partition, β_{ox} 5μm	Diffusion flame energy partition, β_{ox} 20μm	Diffusion flame energy partition, β_{ox} 200μm
0.68	862.4	1048	−0.203	−0.168	0.079	0.604	0.616	0.795
1.21	865.7	1098	−0.201	−0.170	0.023	0.601	0.627	0.800
2.15	868.2	1140	−0.200	−0.177	−0.006	0.616	0.642	0.815
3.83	871.6	1201	−0.201	−0.179	−0.015	0.622	0.695	0.827
6.80	875.6	1280	−0.203	−0.178	−0.026	0.628	0.744	0.824
12.11	879.9	1359	−0.205	−0.175	−0.054	0.672	0.785	0.805

Table 3 Calculated flame lengths for King's 73% AP-HTPB propellants

Pressure, MPa	X^*_D, μm 5μm	X^*_D, μm 20μm	X^*_D, μm 200μm	X^*_{PF}, μm 5μm	X^*_{PF}, μm 20μm	X^*_{PF}, μm 200μm	X^*_{ox}, μm 5μm	X^*_{ox}, μm 20μm	X^*_{ox}, μm 200μm
0.68	2.86	11.45	114.49	6.01	5.07	3.80	20.33	17.36	13.30[a]
1.21	↓	↓	↓	3.10	2.30	1.49	23.59	17.65	11.79
2.15	↓	↓	↓	1.54	0.95	0.63	18.73	11.66	7.97
3.83	↓	↓	↓	0.71	0.43	0.29	10.35	6.33[a]	4.31
6.80	↓	↓	↓	0.30	0.21	0.13	4.47	3.17	2.01
12.11	↓	↓	↓	0.13	0.11	0.02	1.94[a]	1.56	0.81

[a] $\beta_F < 1$ at this and higher pressures.

rates of each pseudopropellant are calculated independently, using the monomodal model, and the aggregate propellant burn rate is a weighted average of the pseudopropellant rates. The present approach is a variation in that it serially builds up the pseudopropellant contributions and determines the burn rate from all of the mass flux and surface area contributions,

$$m_{T,n}\sum_{1}^{n}S_{oj}=(m_{ox}S_{ox})_{j=n}+(m_fS_f)_{j=n}+m_{T,n-1}\sum_{1}^{n-1}S_{oj} \quad (14)$$

$$r=m_{T,n}/\rho_p \quad (15)$$

The first two terms on the right side of Eq. (14) are the mass flow contributions of the oxidizer and binder for the last pseudopropellant. In the calculational procedure that is the coarsest particle size pseudopropellant. The third term is the aggregate mass flow of all finer particle size pseudopropellants. One can view these finer size pseudopropellants in the aggregate as an energetic binder with respect to the coarse particle size.

Surface areas are expressed as in the BDP model. However, an elaboration is required for multimodal propellants because of the use of normalized areas in the BDP model. The expressions for areas are, more fundamentally,

$$S_{oj}=[(\alpha_{ox}/\rho_{ox})_j+(\alpha_f/\rho_f)_j]\times\{\zeta_{fj}+\zeta_{oxj}+3\zeta_{oxj}[(h/D)^2_{Pj}+(h/D)^2_{Nj}]\}$$
$$=V_j\{1+3\zeta_{oxj}[(h/D)^2_{Pj}+(h/D^2_{Nj}]\} \quad (16)$$

$$S_{oxj}=V_j\{\zeta_{oxj}+3\zeta_{oxj}[(h/D)^2_{Pj}+(h/D)^2_{Nj}]\} \quad (17)$$

$$S_{fj}=V_j\zeta_{fj} \quad (18)$$

Dividing Eq. (17) by Eq. (16) provides the (S_{ox}/S_0) of the BDP model. However, use of Eq. (14) requires accounting for the differences in the volume V_j occupied by the different pseudopropellants. The equations for calculating the h/D parameters are the same as for the BDP model; the difference is in the method for determining the binder regression rate, as discussed previously.

The characteristic surface dimension that is used in determining the diffusion height X^*_{Dj} follows the departure from the BDP model indicated previously,

$$b_j=(D_j/\sqrt{6})[1+(\rho_{oxj}/\rho_f)/(O/F)_j] \quad (19)$$

The parameter $(O/F)_j$ depends upon the apportioning of binder to oxidizer among the pseudopropellants. For apportionment by weight, $(O/F)_j$ is a constant equal to the oxidizer/binder ratio.

Variable $(O/F)_j$ concepts are discussed in the Appendix. The scheme maintains a deficiency of other variable surface temperature multimodal models in that continuity of the formulation will not be preserved. Ideas for preserving continuity are included in the Appendix.

Results of Burning Rate Calculations

King's bimodal propellants,[13] a JPL bimodal propellant, and Miller's bimodal and trimodal propellants[15] were utilized to evaluate the model as applied to multimodal AP propellants (nonaluminized, HTPB binder). These propellants are good choices because they encompass a range of size distributions and AP concentrations which test different aspects of the model.

Comparisons of calculated burning rate curves with data for the King and JPL propellants are shown in Fig. 2. The JPL propellant is the intermediate burning rate propellant. Note the wide range of particle sizes covered. The bimodal fine propellant is almost entirely in the regime of diffusion flame control, and predictions continue to be very good as far as that goes. With such fine AP, the reaction distance is an important component of the total diffusion flame height and it will change significantly with solids loading. The ability to predict at both 73 and 82% solids is an important confirmation of this aspect of the theory. The bimodal intermediate propellant is in a mixed regime. The 90 μm pseudopropellant is in the regime of AP flame control with β_{ox} increasing; the 9 μm pseudopropellant transfers from diffusion flame control to AP flame control at about 6.8 MPa. The transition in the data appears more exaggerated than in the model. The bimodal coarse propellant is in the regime where the AP flame controls with β_{ox} increasing, except at high pressure where β_{ox} eventually decreases for the 200 μm pseudopropellant. Viewing the two lower rate propellants, it appears that the coarse pseudopropellants are exerting a greater high-pressure influence than is being predicted by the model.

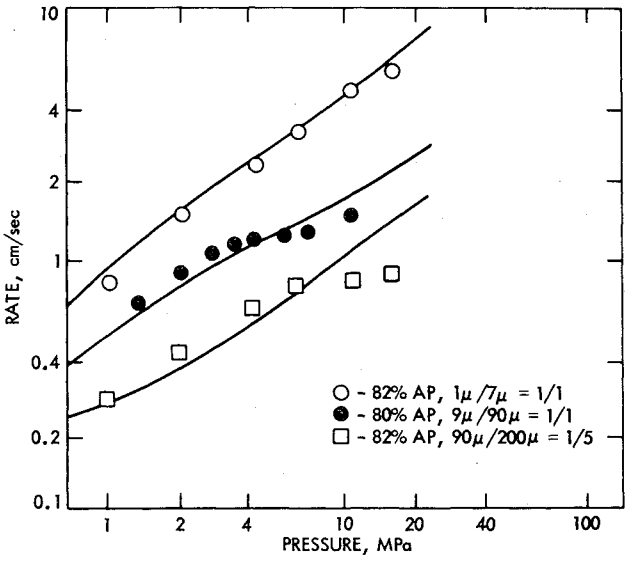

Fig. 2 Comparisons of model and data for bimodal propellants.

Miller's nonaluminized propellants may be classified into two groups: propellants containing 2 μm (or finer) AP and 400 μm AP at a coarse/fine ratio in excess of about 1.5, and all others. The former are referred to as "wide-distribution" propellants. The latter will be called "ordinary" propellants in order to distinguish them.

Evaluation of the model with regard to the ordinary propellants is shown in the form of a comparison plot presented in Fig. 3. Comparisons are displayed for three groups of pressures and three groups of fine AP sizes. Most of these propellants are trimodal, with coarse sizes ranging up to 400 μm. Thus the size distributions cover a broader range than those of Fig. 2. The solids loading is 87.4%, representing a further increase from the propellants of Figs. 1 and 2. Predictions are generally high for the 0.6-2 μm fine size propellants, excellent for the 6 μm propellants, and from excellent to low for the 20 μm propellants. Thus the predicted effect of the fine particle size is somewhat larger than shown by the data. A given error is maintained fairly well over the full pressure range, indicating good predictions of curve shape or pressure exponent. The standard deviation of the predictions is 12.7%.

Calculated pseudopropellant burning rates are shown together with calculated propellant burning rates for two of the Fig. 3 propellants in Table 4. Note that there is not much of an effect of varying the fine AP size until the pressure exceeds 4.3 MPa. The reason is that the reaction distance is the largest component of the diffusion flame height for small AP sizes at low pressures. Note also that the fine AP pseudopropellant exerts the greatest influence on the propellant burning rate with increasing pressure. Comparing the model and data, it appears that the model is overem-

Table 4 Pseudopropellant burning rates: Miller's 87.4% AP (fine/20μm/200μm = 4/3/4)-HTPB propellant

Pressure, MPa	Propellant rate, cm/s		Pseudopropellant rates, cm/s			
	0.6μm fine	6μm fine	0.6μm fine	6μm fine	Intermediate	Coarse
1.36	0.871	0.833	1.217	1.146	0.892	0.335
2.42	1.372	1.262	2.106	1.890	1.232	0.447
4.30	2.131	1.836	3.592	2.962	1.509	0.660
7.66	3.342	2.593	6.002	4.290	1.857	1.036
13.60	5.245	3.536	9.568	5.530	2.667	1.643

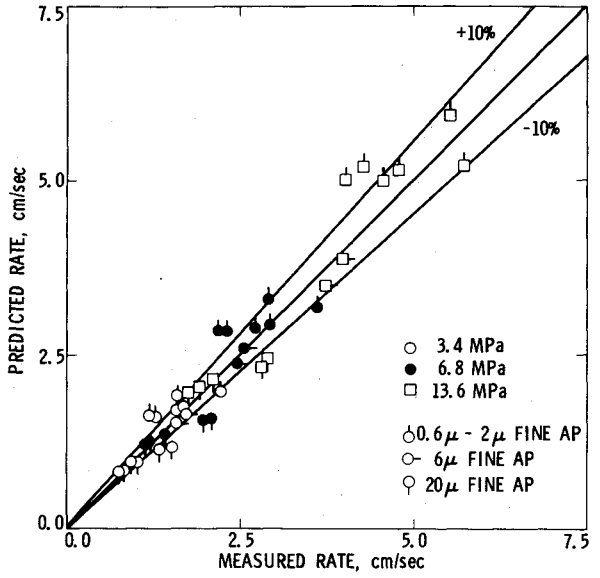

Fig. 3 Comparisons of model and data for Miller's multimodal propellants.

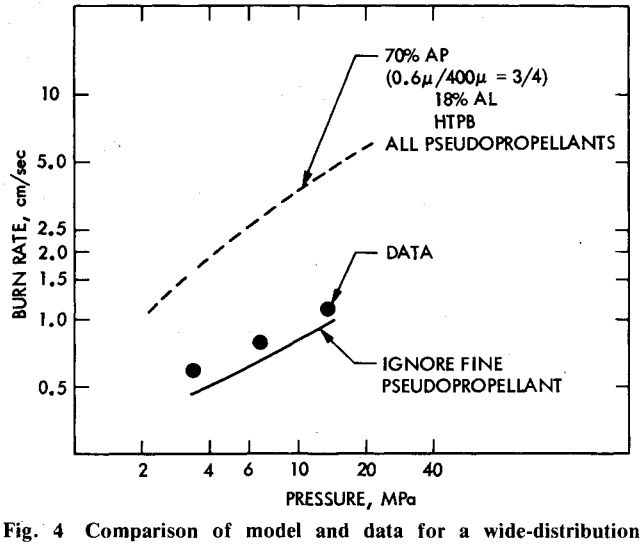

Fig. 4 Comparison of model and data for a wide-distribution propellant.

phasizing the influence of the fine pseudopropellants and underemphasizing the influence of the coarse pseudopropellants. However, the model is correct in that the fine sizes exert the greater influence in these propellants.

The model did not successfully predict the burning rates of the wide-distribution propellants. An example is shown in Fig. 4. An aluminized propellant is used for the illustration because data for the nonaluminized wide-distribution propellants were reported at only one pressure. The presence of the aluminum does not impact the discussion or point to be made because the phenomenon in question originates with the AP and binder alone.[15] It is not just a matter of how the aluminum should be modeled, which is beyond the scope of this paper. Something more than contained in the model is involved with the wide-distribution propellants, whether or not aluminized.

To explore this phenomenon further, calculations were made in which the fine pseudopropellant was omitted from the wide-distribution propellants as though contributing nothing to the combustion. An example of the results obtained is included in Fig. 4. Predictions were improved considerably. Therefore, it appears that the fine pseudopropellant is not contributing to the combustion when it consists of a very small AP size and is combined with a very coarse AP size at coarse/fine ratios above a certain value.

Based on these results, it is concluded that an improved multimodal composite propellant model has been achieved but a major question regarding wide-distribution propellants remains unresolved. The mechanism responsible for the shift in the influence of the fine size component on the burning rate needs to be ascertained in order to develop a more general and consistent model. Further discussion is deferred to the Appendix.

Conclusions

An improved burning rate model has been achieved by incorporating an improved AP monopropellant model, a separate energy balance for the binder in which a portion of the diffusion flame is used to heat the binder, and proper use of the binder regression rate. Improvements have been achieved with regard to predictions of high-pressure burning rates, propellant surface temperatures, and surface structures. The reasons for different burn rate/pressure curve shapes and the effects of particle size and solids loading are better understood. The binder has a more significant role in the combustion than in previous models. There is uncertainty about the high-temperature binder decomposition kinetics and the definition of the diffusion flame shape over the binder to provide the heat feedback. The properties of diffusion flame models should be studied further and experiments with representative diffusion flame burners are recommended.

An improved method for combining component contributions to calculate the burning rates of multimodal propellants has been developed. Predictions for conventional propellants are fairly accurate, but the model appears to weigh the relative contribution of finer AP sizes a bit too heavily. Predictions for a special class of wide-distribution propellants continue to be inaccurate because an apparent suppression of the fine AP contribution is not reflected in the model. Ideas for resolving this problem and for improved multimodal propellant modeling in general are presented in the Appendix.

Appendix: Particle Interaction Modeling

Apportionment of Binder

In the particle interaction model, the apportionment of binder is a function of the particle sizes of the pseudopropellants. Following Beckstead,[5] the apportionment is taken to be on the basis of particle surface area in that the

binder wets particle surfaces,

$$(O/F)_j = (\alpha_{oxj}/\alpha_{fj}) = (D_j/\alpha_f)\Sigma(\alpha_{oxj}/D_j) \quad \text{(A1)}$$

Fine particle sizes tend to be fuel rich and coarse sizes tend to be oxidizer rich.

Flame temperature is shown plotted vs AP concentration, for HTPB propellant, in Fig. A1. A propellant containing 88.5% AP would have a flame temperature of 3050 K and that value would be used in the models which allocate binder by oxidizer weight fraction and therefore do not follow this variable O/F concept. However, following the variable O/F concept, the flame temperatures of particular fuel-rich and oxidizer-rich pseudopropellants can be very low. This represents a considerable loss in available energy and, if nothing else in the model were changed, the predicted burning rates for the pseudopropellants would be so low that the prediction for the overall propellant would be unrealistic. This problem is typical of this form of AP/binder allocation.

Beckstead[6] has argued that the diffusion flame is at a constant temperature, depending upon the stoichiometry, regardless of the propellant formulation. The rationale is that diffusion flames are achieved at stoichiometric proportions of reactants. Thus the flame temperature would be the same for all the pseudopropellants. This argument bears consideration, but was not adopted in this work because it is difficult to accept as a replacement for the thermochemistry. Furthermore, it did not appear that a constant flame temperature would properly reflect either the influence of AP concentration on burning rate or the peculiarities of wide-distribution propellants.

It is possible to remedy the temperature problem with a bookkeeping system to keep track of what is happening to the excess fuel. The fuel that does not enter into the burning of the fine size does not simply disappear to become lost to the system and unaccountable in the burning of the coarser sizes. Clearly, this excess fuel continues to diffuse and must be available for the combustion occurring about the next coarser size, and so on. It is in this manner that the fuel can be consumed to the extent possible in actual multimodal propellants.

The fuel that is actually burned in a given pseudopropellant may be given by

$$\alpha_{frj} = \alpha_{oxj}/\phi \quad \text{(A2)}$$

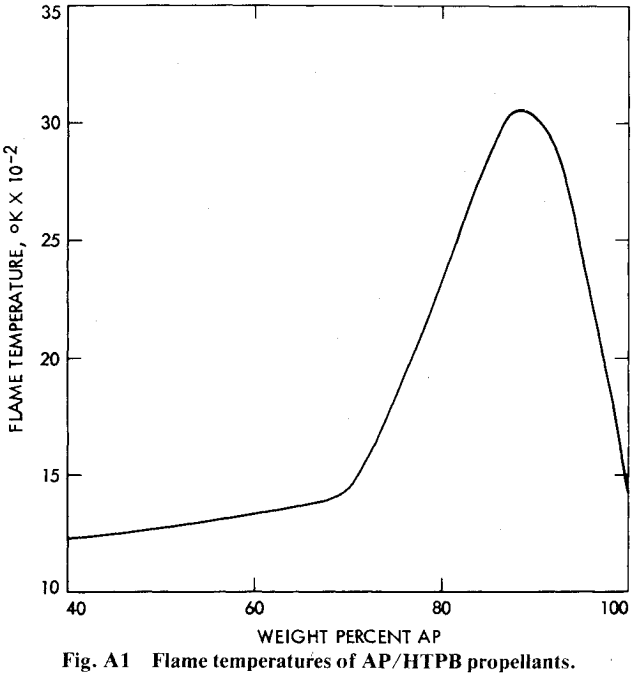

Fig. A1 Flame temperatures of AP/HTPB propellants.

The amount of fuel that is available to react in the given pseudopropellant is actually the sum of the binder allocated to that pseudopropellant and the excess fuel coming from the prior pseudopropellant,

$$\alpha^*_{fj} = \alpha_{oxj}/(O/F)_j + \alpha_{fe(j-1)} \quad \text{(A3)}$$

Thus, the excess fuel that will go to the succeeding pseudopropellant (next coarser size) will be

$$\alpha_{fej} = \alpha_{oxj}/[1/(O/F)_j - 1/\phi] + \alpha_{fe(j-1)} \quad \text{(A4)}$$

Note that where $(O/F)_j > \phi$, as is the case for coarser sizes, some of the excess fuel coming from the fine size is going to be consumed such that a lesser excess will be available to the coarsest size and the final excess will be that of the aggregate propellant. This is a much more realistic approach.

An effective O/F ratio for the pseudopropellant can now be defined as

$$(O/F)^*_j = \alpha_{oxj}/\alpha^*_{fj} \quad \text{(A5)}$$

The pseudopropellant containing the finest AP is the only one that remains unchanged. All of the others have more fuel available. The propellant energy is thereby restored in the coarser sizes.

This approach affords the opportunity to predict more realistic burning rates and account for wide distribution phenomena. It appears that the fine AP pseudopropellant operates as a relatively cool, fuel-rich system and in extreme formulations it may be too cool to operate effectively. A common feature of pseudopropellants containing very fine AP is that the reaction distance is a major part of the diffusion flame height at pressures of interest. That is a basic reason for the relatively high-pressure exponent of fine AP propellants, and a saturation of the burning rate increase below a certain AP size.[2] The reaction distance is sensitive to the flame temperature in the current model, which is an important factor in predicting the burning rates of ordinary propellants containing fine AP over the range 73-87% solids. Consequently, a possible mechanism for surpressing the fine AP would be a lowering of the flame temperature so as to substantially increase the reaction distance. According to Eq. (A1), the suppression would be promoted by decreasing fine size, increasing coarse size, and increasing coarse/fine ratio. These trends are consistent with the data.

Application of this model to two of the propellants discussed in the main text is shown in Fig. A2. It is observed that the wide-distribution propellant is now predicted quite well, but the ordinary propellant is not predicted well in the regime of diffusion flame control. The difference in the prediction for the wide-distribution propellant reflects a drop in the fine pseudopropellant flame temperature from 2875 to 1503 K. The fine pseudopropellant is now contributing very little to the combustion, but it is more than zero. The difference in the prediction for the ordinary propellant also reflects a drop in the fine pseudopropellant flame temperature, but it does not have as great an impact because it is not as large and because the 90 μm "coarse" size is fine enough to better maintain the burn rate level. Thus a "narrow distribution" propellant is less sensitive to this mechanism.

As developed thus far, the particle interaction model is deficient in predicting the burning rates of the ordinary propellants. Thus more work is needed to bridge the gap between ordinary and wide-distribution propellants. It is considered that the apportionment of binder approach presented is a good beginning.

Pseudopropellant Buildup and Preservation of Continuity

Renie[16] performed a series of calculations in which the binder allocation as a function of particle size was allowed to be a floating parameter, and determined the value required to

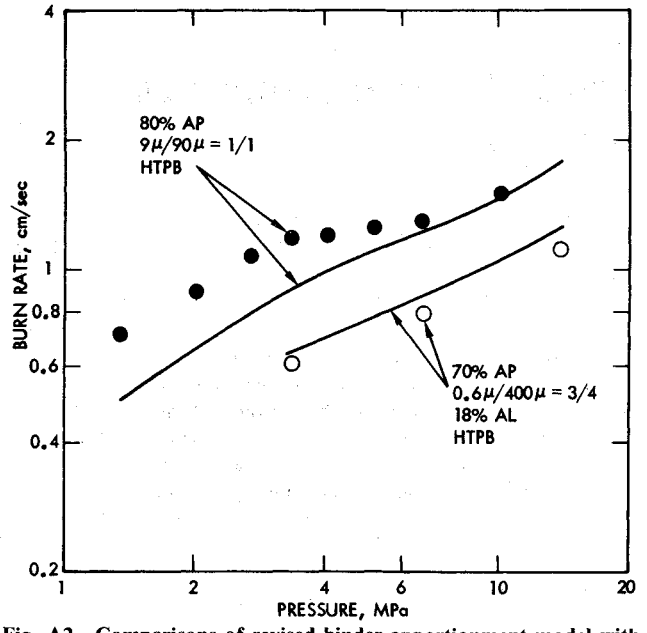

Fig. A2 Comparisons of revised binder apportionment model with data.

match burning rate data for a set of formulations at one pressure. This approach is not satisfying because of the wide variability obtained and the lack of some basic principle that would determine such variable allocations.

One principle that could provide the determination is the preservation of formulation continuity. It can be argued that the pseudopropellants implicitly adjust as to their binder allocations such that the continuity of the formulation is preserved. This could be imposed as a constraint in the model, and the particular allocation would be left as an unknown to be iterated upon. This is readily envisioned for a bimodal propellant, but something more would be needed for a trimodal propellant. For a trimodal propellant, the added dimension can be provided by allocating not only binder but also the pseudopropellant as unknowns. In other words, the fine pseudopropellant would itself be allocated between the other two oxidizer sizes; it "wets" the coarse as well as the intermediate size. The result would be constrained to match the oxidizer ratios and overall oxidizer/binder ratio of the formulation. Although this approach would complicate the bookkeeping, it is recommended for future exploration because propellants probably do adjust themselves this way during burning.

Flame Interactions

By flame interaction, it is meant that the diffusion flame structure from one pseudopropellant enters directly into the competing flame process and/or energy balance regarding another pseudopropellant. In the model developed thus far, each diffusion flame heats only the associated oxidizer and assigned portion of binder. It is now proposed that the diffusion flame associated with a coarser particle size may contribute to the heating of the finer size pseudopropellant. It appears to be a viable approach to supplying more heat to the fine pseudopropellant so as to raise its burning rate, compensating for the low temperature and fuel richness, and perhaps thereby bridge the gap between ordinary and wide-distribution propellants. However, it would produce a much more complicated model because of the multiplicity of couplings involved. Nevertheless, it is recommended for future exploration.

Acknowledgments

This work was sponsored by the Air Force Office of Scientific Research, Support Agreements AFOSR-ISSA-79-0016 and AFOSR-ISSA-80-0017, through an agreement with the National Aeronautics and Space Administration. The authors hereby express their appreciation to C.F. Price of the Naval Weapons Center and M.W. Beckstead of Brigham Young University for helpful discussions concerning the modeling of monopropellants and composite propellants.

References

[1] Beckstead, M.W., Derr, R.L., and Price, C.F., "A Model of Composite Solid Propellant Combustion Based on Multiple Flames," *AIAA Journal*, Vol. 8, Dec. 1970, pp. 2200-2207.

[2] Cohen, N.S., "Review of Composite Propellant Burn Rate Modeling," *AIAA Journal*, Vol. 18, March 1980, pp. 277-293.

[3] Price, C.F., Boggs, T.L., and Derr, R.L., "The Steady-State Combustion Behavior of Ammonium Perchlorate and HMX," Paper 79-0164 presented at AIAA 17th Aerospace Sciences Meeting, Jan. 1979.

[4] Beckstead, M.W., Derr, R.L., and Price, C.F., "The Combustion of Solid Monopropellants and Composite Propellants," *Thirteenth Symposium (International) on Combustion*, The Combustion Institute, Pittsburgh, Pa., 1971, pp. 1047-1056.

[5] Beckstead, M.W., "A Model for Solid Propellant Combustion," *14th JANNAF Combustion Meeting*, CPIA Publication 292, Vol. I, Dec. 1977, pp. 281-306.

[6] Beckstead, M.W., "A Model for Solid Propellant Combustion," *Eighteenth Symposium (International) on Combustion*, The Combustion Institute, Pittsburgh, Pa., 1981, pp. 175-185.

[7] Price, C.F. and Boggs, T.L., Letter Memorandum 388-299-79, U.S. Naval Weapons Center, China Lake, Calif., Aug. 1979.

[8] Burke, S.P. and Schumann, T.E.W., "Diffusion Flames," republished in *First and Second Symposiums on Combustion*, The Combustion Institute, Pittsburgh, Pa., 1965, pp. 2-11.

[9] Beckstead, M.W., private communications, Brigham Young University, Provo, Utah, 1981.

[10] Fenn, J.B., "A Phalanx Flame Model for the Combustion of Composite Solid Propellants," *Combustion and Flame*, Vol. 12, June 1968, pp. 201-216.

[11] Price, E.W., Handley, J.C., Panyam, R.R., Sigman, R.K., and Ghosh, A., "Combustion of Ammonium Perchlorate-Polymer Sandwiches," *AIAA Journal*, Vol. 19, March 1981, pp. 380-386.

[12] King, M.K., "Model for the Steady State Combustion of Unimodal Composite Solid Propellants," Paper 78-216 presented at AIAA 16th Aerospace Sciences Meeting, Jan. 1978.

[13] King, M.K., "A Model of the Effects of Pressure and Crossflow Velocity on Composite Propellant Burning Rate," Paper 79-1171, 15th AIAA/SAE/ASME Joint Propulsion Meeting, June 1979.

[14] Cohen, N.S., Fleming, R.W., and Derr, R.L., "Role of Binders in Solid Propellant Combustion," *AIAA Journal*, Vol. 12, Feb. 1974, pp. 212-218.

[15] Miller, R.R., et al., "Control of Solids Distribution in HTPB Propellants," Hercules Inc., Cumberland, Md., AFRPL-TR-78-14, April 1978.

[16] Renie, J.P. and Osborn, J.R., "An Implicit Flame Interaction Combustion Model," *15th JANNAF Combustion Meeting*, CPIA Publication 297, Vol. II, Feb. 1979, pp. 217-240.